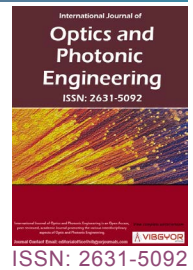


# Optical and Dielectric Properties for the Determination of Gap States of the Polymer Conductor: Polypyrrol



**C Belabed<sup>1\*</sup>, A Tab<sup>2</sup>, B Belhamedi<sup>3</sup> and N Benrakaa<sup>1</sup>**

<sup>1</sup>Laboratory of Materials Physic, Faculty of Physic, USTHB, Algiers, Algeria

<sup>2</sup>Laboratory of Chromatography, Faculty of Chemistry, USTHB, Algiers, Algeria

<sup>3</sup>Laboratory of Physical and Chemical Study of Materials and Applications in the Environment, Faculty of Chemistry, USTHB, Algiers, Algeria

## Abstract

The polypyrrole is a conducting polymer prepared by chemical route. The diffuse reflectance measured in the wavelength range (300-2500 nm) permitted to calculate the refractive index (n), extinction coefficient (k), dissipation factor ( $\tan \delta$ ) and relaxation time ( $\tau$ ). The optical band gap ( $E_g$ ) was evaluated from the dielectric and conductivity properties, its value (1.01 eV) was confirmed by using the Tauc relation.

## Keywords

Polymer conductor, Polypyrrol, Optical dispersion parameters, Dielectric properties, Optical constants

## Introduction

The development of electronic devices light, flexible also small-size and rechargeable has increased during recent years [1-3]. In this respect, the polymer conductors have attracted a great interest from both academic and technical point of view over the last decade [4-6]. Such materials not only work in a similar way to inorganic semi-conductors (SCs) but also have additional advantages like environmental friendliness, facile synthesis and light weight [7]. Moreover, organic materials show higher conductivity due to the itinerant electron on conjugated system compared to the inorganic SCs [8]. The main advantage with organic materials is that both the structure and properties can be tallo-

ried, with inherent ultra-fast time and large optical susceptibilities, needed characteristics of the modern technological requirements [9].

Among the candidates, Polypyrrol (PPy) is an emergent material because it has interesting optical properties [10] which are essential for optoelectronic applications [11]. The optical constants of the semiconductors play an important from both a fundamental and technological points of view. The refractive index is closely related to the electronic polarizability of ions and local field inside the materials [12]. With this in mind, we have prepared PPy by chemical route and investigated the optical and dielectric properties.

\*Corresponding author: C Belabed, Laboratory of Materials Physic, Faculty of Physic, USTHB, BP 32 El-Alia, 16111, Algiers, Algeria, Tel: +213-21-24-79-55, Fax: +213-21-24-80-08

Accepted: August 26, 2020; Published: August 28, 2020

Copyright: © 2020 Belabed C, et al. This is an open-access article distributed under the terms of the Creative Commons Attribution License, which permits unrestricted use, distribution, and reproduction in any medium, provided the original author and source are credited.

Belabed et al. *Int J Opt Photonic Eng* 2020, 5:025

ISSN 2631-5092



9 772631 509009

## Experimental

The polypyrrol (PPy) was prepared by chemical route, from the pyrrole monomer which was purified to remove the impurities. The distilled pyrrole (0.2 M) was dissolved in a mixture of water/ethanol (1:1), FeCl<sub>3</sub> (0.1 M) was slowly added to the solution under stirring for 24 h at room temperature. The black precipitate PPy was filtered, thoroughly washed with water and ethanol mixture and dried at 323 K for 24 h under vacuum.

## Results and Discussion

### Refractive index dispersion

The reflectance measurement of PPy was used for determination of the refractive (*n*) and extinction (*k*) indices using the complex optical refraction [13]:

$$\hat{n} = n(\lambda) + ik(\lambda) \tag{1}$$

Where, *n* and *k* are the real and imaginary parts respectively. The coefficient (*k*) is calculated in terms of absorption coefficient ( $\alpha$ ) and light wavelength ( $\lambda$ ) from the well-known relation [13,14]:

$$k = \frac{\alpha\lambda}{4\pi} \tag{2}$$

While the refractive index is determined by the relation [12]:

$$n(\lambda) = \frac{(1+R(\lambda)) + \sqrt{4R(\lambda) - (1-R(\lambda))^2 K(\lambda)^2}}{1-R(\lambda)} \tag{3}$$

Figure 1 shows the variations of *n* and *k* versus the wavelength ( $\lambda$ ), in the UV- visible region, the coefficient *k* increases drastically to reach a maximum at 760 nm and this indicates that a large fraction of the light is lost. On the other hand, the refractive index *n* decreases with increasing  $\lambda$  indicating a best optical characteristic of PPy with promising applications in the visible region. Above which *k* decreases up to 1600 nm and remains nearly constant and this indicates a maximum light absorption in the IR region ( $\lambda > 760$  nm). While for the refractive index increases, and its value has doubled in the IR region.

### Dielectric study

The interaction electron/photon is expressed by the complex dielectric constant ( $\epsilon$ ) which is proportional to the polarizability of PPy and comprises the real ( $\epsilon_r$ ) and imaginary parts ( $\epsilon_i$ ), they are determined from the coefficients *n* and *k* by using the following relations [15]:

$$\epsilon_r = n^2 + k^2 \tag{4}$$

$$\epsilon_i = 2nk \tag{5}$$

The dependence of  $\epsilon_r$  and  $\epsilon_i$  versus *h* $\nu$  are illustrated in Figure 2. The extrapolation of the straight line to the real and imaginary curves of the dielectric constant to the x-axis yields an optical gap *E*<sub>gof</sub> ~ 0.6 eV.

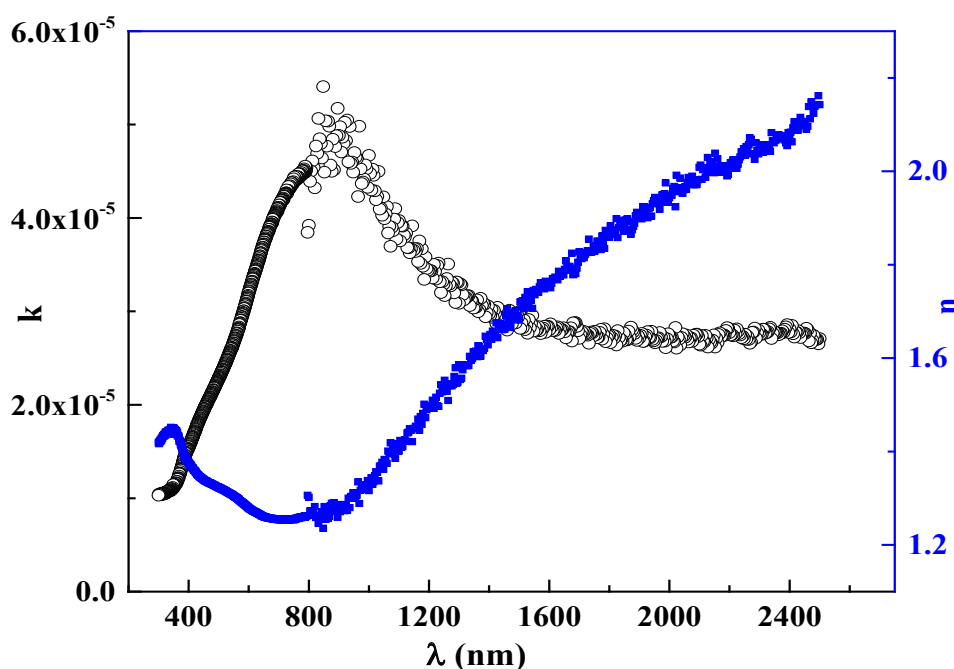
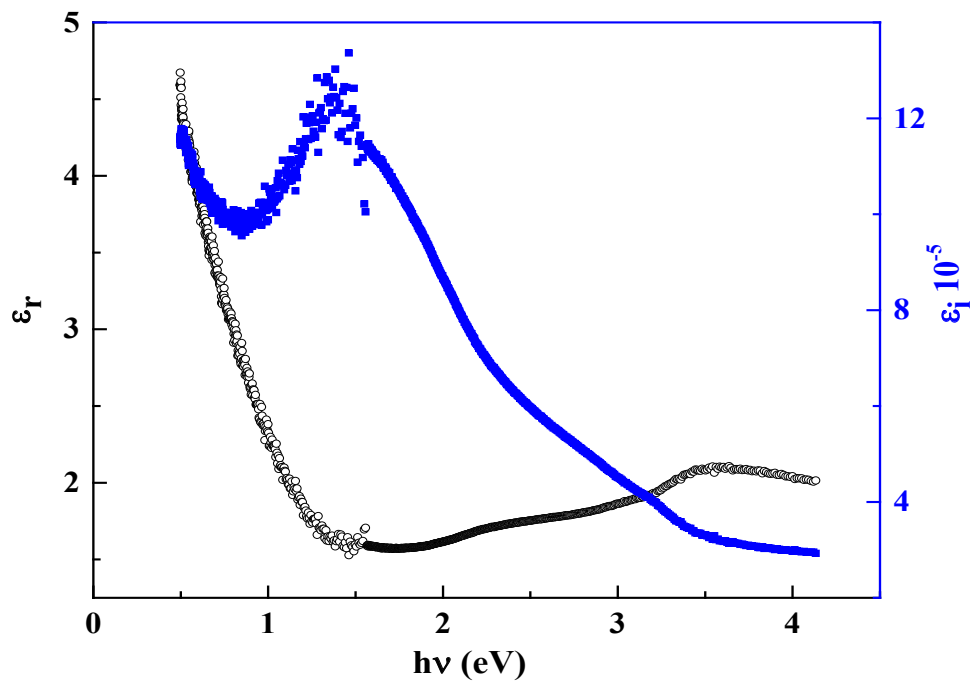
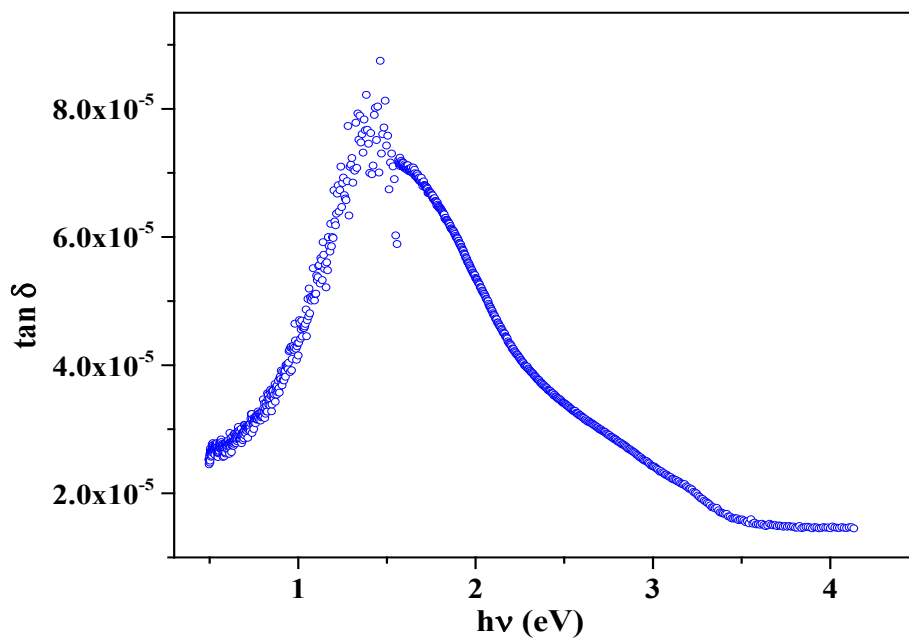


Figure 1: Extinction coefficient and Refractive index against wavelength for PPy.



**Figure 2:** Real and imaginary parts of the dielectric constant as function of photon energy of PPy.



**Figure 3:** Dependence of the dissipation factor  $\tan \delta$  on the photon energy for PPy.

In physics, the measurement of loss-rate of power of a mechanical mode in oscillation is expressed by the dissipation factor. In polymer conductors, the electrical power lost in the form of heat and the dissipation factor is given by the following relation [16]:

$$\tan \delta = \frac{\epsilon_i}{\epsilon_r} \tag{6}$$

Figure 3 shows the profile  $\tan \delta$  vs.  $h\nu$ . In the range (0.3-1.4 eV),  $\tan \delta$  increases significantly indicating a radiative motor effect and this means that the radiative effect dominates the developed physics. By contrast,  $\tan \delta$  decreases above 1.4 eV and this implies that the energies are suitable, in agreement with the  $k$  values. Different quantities were used to characterize the optical properties of

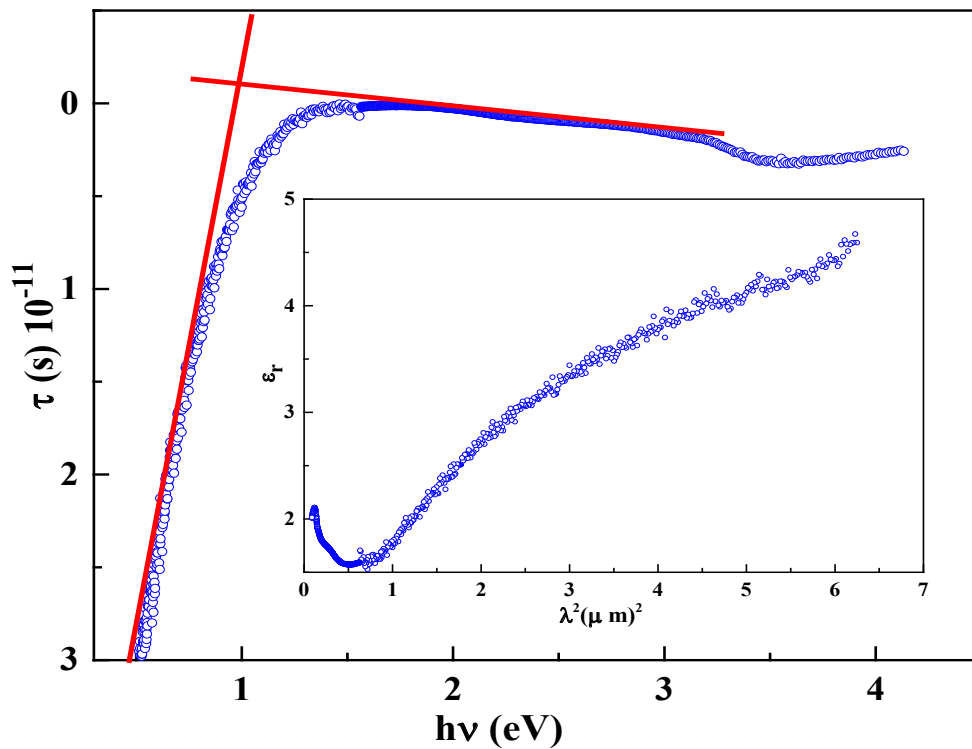


**Figure 4:** Dependence of the dielectric relaxation time  $\tau$  on the photon energy  $h\nu$ . Inset: The  $\epsilon_r$  vs.  $\lambda^2$ .

PPy among which the dielectric relaxation time ( $\tau$ ), evaluated from the relation [15]:

$$\tau = \left| \frac{\epsilon_\infty - \epsilon_r}{\omega \epsilon_i} \right| \tag{7}$$

Where  $\epsilon_\infty$  is the infinite dielectric constant which can be easily deduced when the incident-energy tends to infinity, and is the smallest value of  $\epsilon_r$  ( $\epsilon_\infty = 1.54$ ) (Figure 4 inset). Figure 4 shows the dielectric relaxation time as a function of  $h\nu$  for PPy. The cross-point between the tangent of the plot of lower and higher values of the energy ( $h\nu$ ) of the calculated relaxation time to the x-axis. Permit to evaluate the band-to-band absorption, which corresponds to the optical bandgap ( $E_g \sim 1.01$  eV).

The relation between the coefficient ( $n$ ) and lattice dielectric constant ( $\epsilon_L$ ) is given by [16]:

$$n^2 = \epsilon_L - \left( \frac{e^2}{\pi c^2} \times \frac{N}{m^*} \right) \lambda^2 \tag{8}$$

Where,  $e$  is the electronic charge and  $c$  is the velocity of light and  $N/m^*$  the ratio of the carriers concentration to the effective mass. The plot  $n^2$  versus  $\lambda^2$  (Figure 5) is linear in conformity with Eq. (8). The  $\epsilon_L$  values (1.57) can be easily deduced by extrapolating the plots to  $\lambda^2 = 0$  while the ration  $N/m^*$  is determined from the slope of the graph. The values

of  $\epsilon_\infty$  and  $\epsilon_L$  are close to each due to no carrier contribution.

### Optical and electrical conductivity

The conductivity is an important parameter to know in the behavior of materials. The optical ( $\sigma_{opt}$ ) and electrical ( $\sigma_e$ ) conductivities of PPy are given by the relations [15,16]:

$$\sigma_{opt} = \frac{\alpha n C}{4\pi} \tag{9}$$

$$\sigma_e = \frac{2\lambda \sigma_{opt}}{\alpha} \tag{10}$$

Figure 6 shows graphs the  $\sigma_{opt}$  and  $\sigma_e$  as a function of ( $h\nu$ ). At first sight,  $\sigma_e$  decreases with increasing the energy  $h\nu$ , and  $\sigma_{opt}$  increases with augmenting the photon energy. The peak at 1.72 eV this implies that PPy has good optical properties in the visible region and the conduction of photons is a dominant mechanism instead of the electrical conduction. The cross-point between the curves  $\sigma_{opt}$  and  $\sigma_e$  allows evaluating the optical band gap  $E_g$  ( $\sim 0.95$  eV) in good agreement with our previous results [8].

### Determination of the optical band gap

The relation between the absorption coefficient ( $\alpha$ ) and incident photon energy ( $h\nu$ ) provides valu-

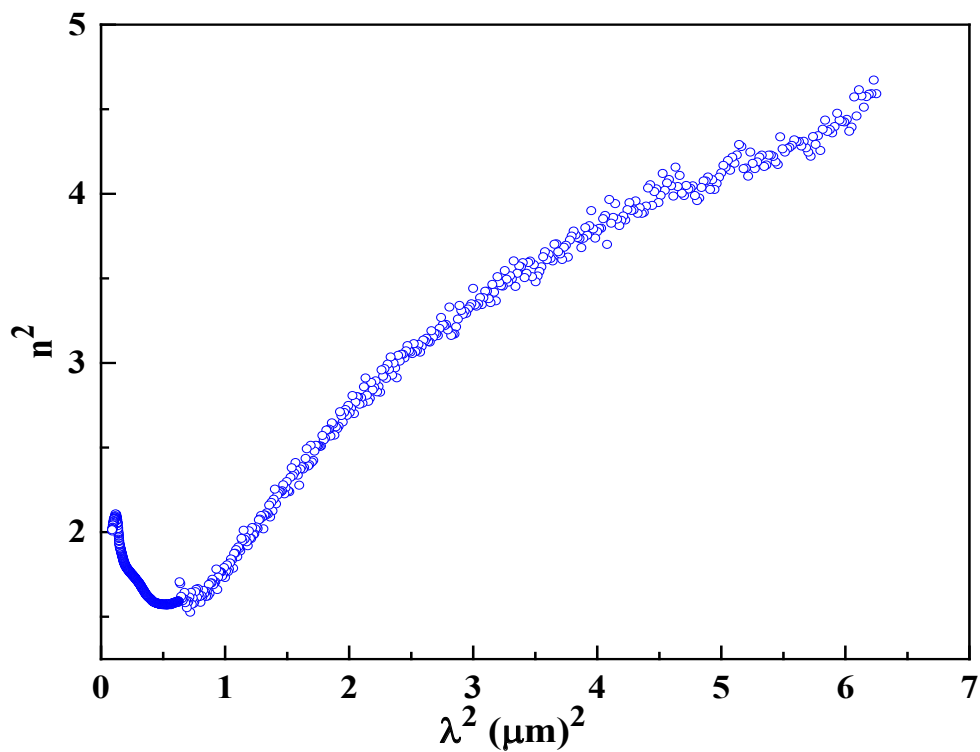


Figure 5: Plot of  $n^2$  versus  $\lambda^2$  of PPy.

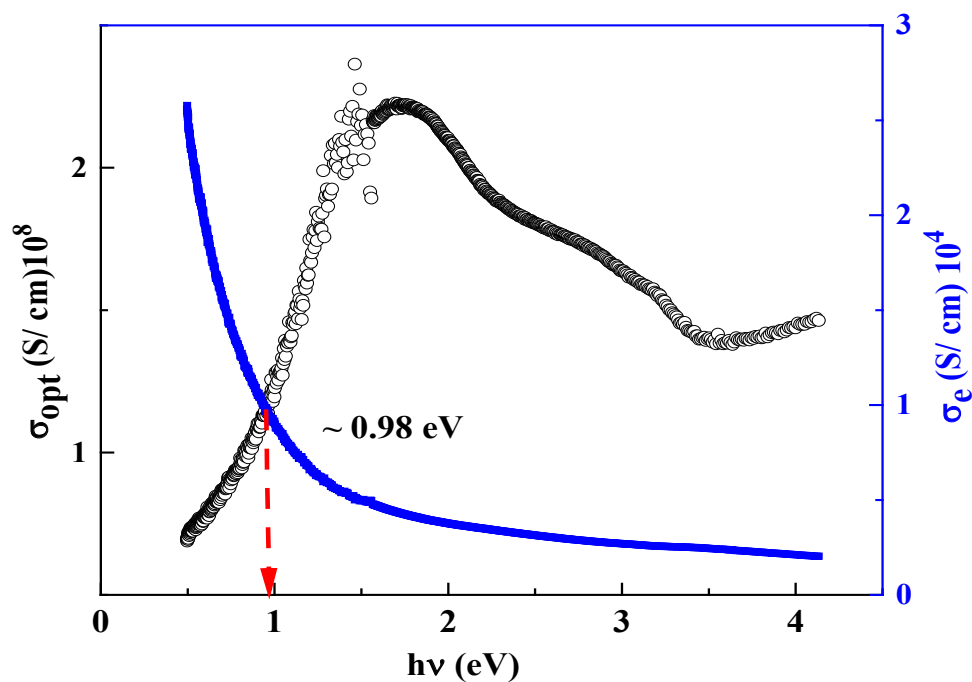


Figure 6: Optical and electric conductivity against photon energy for PPy.

able information about the optical gap by using the relation [17]:

$$(\alpha hv)^m = Const \times (hv - E_g) \tag{11}$$

The exponent  $m$  depends on the transition type,  $m = 2$  and  $1/2$  for direct or indirect transitions re-

spectively. The intercepts of the linear plot  $(\alpha hv)^m$  with the  $hv$ -axis of PPy yield, direct and indirect transitions at 0.42 and 1.01 eV respectively (Figure 7 and Figure 8), in good agreement with the values obtained previously. The study has been the subject of continuing interest on the hero-system PPy/

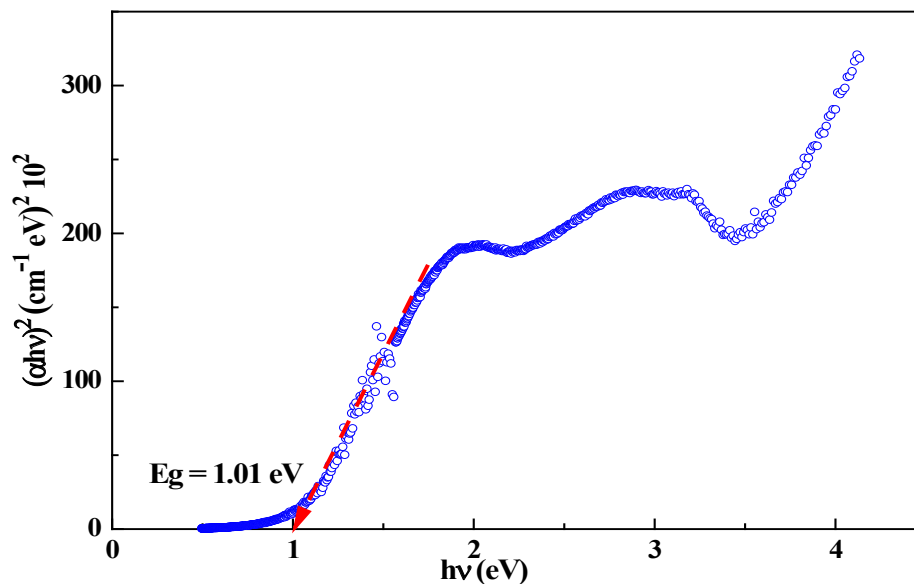


Figure 7: Direct optical transitions of PPy.

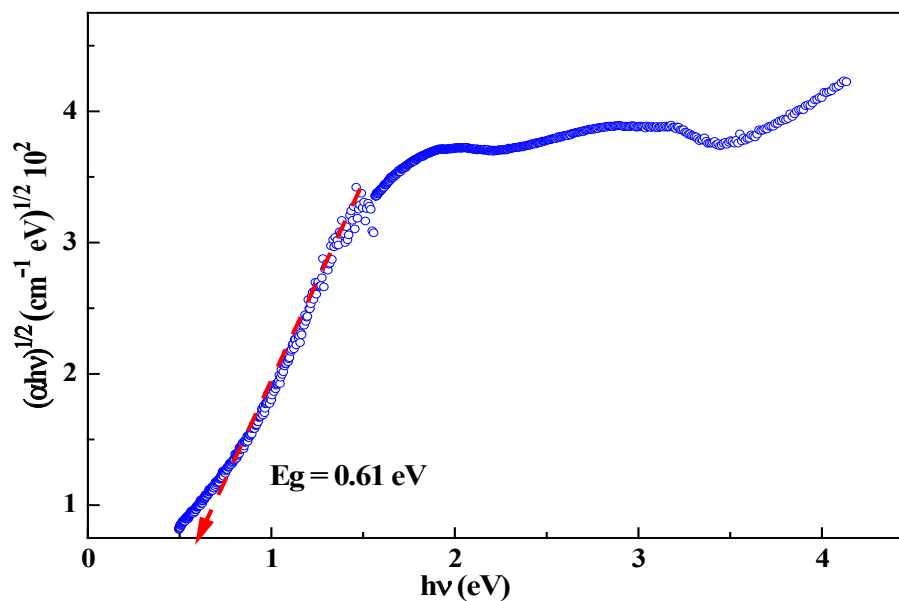


Figure 8: Indirect optical transitions of PPy.

TiO<sub>2</sub>; the results are satisfactory and the work will be published in a near future.

## Conclusion

The polypyrrol was prepared by chemical route, and the electric and dielectric properties were investigated. The peak in the spectral distribution of the refractive index and the dielectric relaxation time corresponds to the fundamental absorption edge. The optical band gap was evaluated by different methods, the obtained values are almost close to that determined by diffuse reflectance.

## Acknowledgments

The authors wish to express their thanks for the financial support from the Directorate general of Scientific Research and technological Development (DGRST, Algeria).

## References

1. R Kandulna, R Choudhary (2017) Robust electron transport properties of PANI/PPY/ZnO polymeric nanocomposites for OLED applications. *Optik* 144: 40-48.
2. M Majhi, R Choudhary, P Maji (2017) HCl protonated

- polymeric PANI-ZnS nanocomposites and measurement of their robust dielectric, optical and thermal performance. *Optik* 136: 181-191.
3. S Krishnaswamy, V Ragupathi, S Raman, P Panigrahi, G Nagarajan (2019) Optical properties of P- type polypyrrole thin film synthesized by pulse laser deposition technique: Hole transport layer in electroluminescence devices. *Optik* 194: 163034.
  4. S Sharma, S Misra (2002) Optimization of conducting polymer thin film optical and electrical waveguides. *Optik* 113: 351-353.
  5. A Alyamani, K Ibnaouf, O Yassin, M AlSalhi, Z Fekkai, et al. (2016) Spectral, electrical and morphological properties of spin coated MEH-PPV and cresyl violet blended thin films for a light emitting diode. *Optik* 127: 2331-2335.
  6. N Mustapha, Z Fekkai, A Alkaoud (2016) Enhanced efficiency of organic solar cells based on (MEH-PPV) with graphene and quantum dots. *Optik* 127: 2755-2760.
  7. C Belabed, N Haine, Z Benabdelghani, B Bellal, M Trari (2014) Photocatalytic hydrogen evolution on the hetero-system polypyrrol/TiO<sub>2</sub> under visible light. *Int J Hydrogen Energy* 39: 17533-17539.
  8. C Belabed, G Rekhila, M Doulache, B Zitouni, M Trari (2013) Photo-electrochemical characterization of polypyrrol: Application to visible light induced hydrogen production. *Sol Energy Mater Sol Cells* 114: 199-204.
  9. A Ashery, MA Salem, A Farag (2018) Optical and electrical performance of polypyrrol thin films and its hybrid junction applications. *Optik* 172: 302-310.
  10. J Chandrasekaran, D Nithyaprakash, B Punithaveni, L Sasikumar, KB Ajjan, et al. (2013) Study of optical, dielectric and optoelectronic properties of dodecylbenzene sulfonic acid doped polypyrrole. *Optik* 124: 2057-2061.
  11. Sk Basha, G Sundari, K Kumar, K Rao, MC Rao (2018) Preparation and characterization of ruthenium based organic composites for optoelectronic device application. *Optik* 164: 596-605.
  12. C Belabed, B Bellal, A Tab, K Dib, M Trari (2018) Optical and dielectric properties for the determination of gap states of the polymer semiconductor: Application to photodegradation of organic pollutants. *Optik* 160: 218-226.
  13. Z Serbetc, HM El-Nasser, F Yakuphanoglu (2012) Photoluminescence and refractive index dispersion properties of ZnO nanofibers grown by sol-gel method. *Spectrochimica Acta Part A: Molecular and Biomolecular Spectroscopy* 86: 405-409.
  14. P Dinakaran, S Kalainathan (2013) Studies on the optical and mechanical properties of organic nonlinear optical 1-(4-fluorostyryl)-4-nitrostilbene (FNS) single crystal. *Optik* 12: 5111-5115.
  15. GB Sakr, IS Yahia, M Fadel, SS Fouad, N Romcevic (2010) Optical spectroscopy, optical conductivity, dielectric properties and new methods for determining the gap states of CuSe thin films. *J Alloy Compd* 507: 557-562.
  16. MM El-Nahassa, AAM Faraga, EM Ibrahim, S Abd-El-Rahman (2004) Structural, optical and electrical properties of thermally evaporated Ag<sub>2</sub>S thin films. *Vacuum* 72: 453-460.
  17. N Doufar, M Benamira, H Lahmar, M Trari, I Avramova, et al. (2020) Structural and photochemical properties of Fe-doped ZrO<sub>2</sub> and their application as photocatalysts with TiO<sub>2</sub> for chromate reduction. *J Photochem Photobiol A: Chem* 386: 112105.